Femtosecond pump/probe photoelectron spectroscopy of isolated C_{60} negative ions

Oli T. Ehrler
Institut für Physikalische Chemie, Universität Karlsruhe, Kaiserstrasse 12, D-76128 Karlsruhe, Germany

Ji Ping Yang
Institut für Nanotechnologie, Forschungszentrum Karlsruhe, P.O. Box 3640, D-76021 Karlsruhe, Germany and Department of Applied Physics, Hefei University of Technology, Hefei 230009, China

Christof Hättig[a)]
Institut für Nanotechnologie, Forschungszentrum Karlsruhe, P.O. Box 3640, D-76021 Karlsruhe, Germany

Andreas-N. Unterreiner and Horst Hippler
Institut für Physikalische Chemie, Universität Karlsruhe, Kaiserstrasse 12, D-76128 Karlsruhe, Germany

Manfred M. Kappes[b)]
Institut für Physikalische Chemie, Universität Karlsruhe, Kaiserstrasse 12, D-76128 Karlsruhe, Germany and Institut für Nanotechnologie, Forschungszentrum Karlsruhe, P.O. Box 3640, D-76021 Karlsruhe, Germany

(Received 18 May 2006; accepted 6 July 2006; published online 21 August 2006; publisher error corrected 22 August 2006)

We have measured pump/probe photoelectron spectra of mass-selected, near room temperature C_{60}^- in the gas phase. The lifetime of the vibrationally excited $\tilde{B}^-(^2E_g)$ state at a calculated energy of 1.26 eV was found to be $\tau=2.2\pm0.2$ ps. The dominant decay process corresponds to intramolecular radiationless transitions into ground state C_{60}^-. This is in contrast to C_{60} for which pumping at the absorption onset (1.95 eV) leads to predominantly intersystem crossing. © *2006 American Institute of Physics*. [DOI: 10.1063/1.2244557]

I. INTRODUCTION

Due to its unique symmetry and stability, buckminsterfullerene has rapidly become one of the best studied large polyatomic molecules. Correspondingly, C_{60} is often used as a model system with which to probe a variety of fundamental chemical physics issues. One area of intense study has been time resolved electronic spectroscopy. Resulting data can help to understand intramolecular energy redistribution in the large molecule limit. Specifically, excitation of C_{60} at an energy just above its absorption onset near 1.95 eV is associated with the population of up to three close lying excited singlet states. Transient spectroscopy shows that the lowest of these singlets (S_1) decays dominantly by intersystem crossing (ISC) to a nearly resonant triplet state(s). Some S_1 fluorescence is also observed, but its lifetime of ca. 1–1.5 ns reflects primarily the ISC rate. This also sets an upper limit on the rate of nonradiative S_0-S_1 relaxation.

Most time resolved measurements have probed C_{60} in condensed phase[1–7] and as such are influenced by poorly understood coupling to the matrix to an unknown extent. Furthermore, in the study of thin films photoinduced degradation can cause severe problems, as systematically explored by Fleischer *et al.*[8] Comparison to transient spectroscopy of *isolated* (gas phase) molecules can therefore provide useful input. However, such measurements are hampered by much lower sample densities typically requiring ionization/charge detection to ensure sufficient sensitivity. As yet there is only a patchwork of transient spectroscopy results for gas-phase C_{60}—using mainly photoionization and photoelectron spectroscopies. Recent measurements with laser systems of different pulse lengths have provided first insight into the decay mechanisms and time scales of electronic excitations.[9–12] After irradiation with pulses of 500 fs length at a wavelength of 790 nm and laser fluences on the order of 10 J/cm^2, thermal emission of electrons occurs. The high electron temperature and the lack of fragmentation indicate that emission derives exclusively from a hot electronic subsystem. Contrary to this, the kinetic energy distribution of electrons emitted after irradiation with a 5 ps laser pulse of the same fluence is substantially colder. This, as well as the strong fragmentation and delayed ionization also observed, indicates partial conversion of electronic energy into vibrational degrees of freedom between the absorption of successive photons. As laser pulse lengths are not easily variable and the experiments cited typically involve the absorption of several photons, assignment of lifetimes to distinct electronic states was so far not possible under isolated conditions.

C_{60}^- has a vertical electron detachment energy nearly 5 eV lower than the ionization energy of C_{60}. This makes C_{60}^- more readily accessible to *two-color* pump/probe photoelectron spectroscopy using femtosecond lasers, a method which

[a)]Present address: Lehrstuhl für Theoretische Chemie, Ruhr-Universität Bochum, Universitätsstraße 150, D-44801 Bochum, Germany.
[b)]Fax: ++49-721-608-7232. Electronic mail: manfred.kappes@chemie.uni-karlsruhe.de

 © 2006 American Institute of Physics

Downloaded 23 Aug 2008 to 134.147.252.238. Redistribution subject to AIP license or copyright; see http://jcp.aip.org/jcp/copyright.jsp

provides a much clearer view of excited state dynamics than one-color (multiphoton) measurements. Below, we report the first transient spectroscopy measurements on C_{60}^- prepared and probed in ion beams at near room temperature. Using the first harmonic of a Ti:Sa femtosecond laser system (775 nm) as the pump, and the frequency doubled output (388 nm) as the probe pulse, we observe a transient two-color/two-photon signal. This is associated with detachment from the first electronically excited doublet state. The measured lifetime and associated relaxation mechanisms are discussed in terms of time-dependent density functional theory calculations of electronically excited states.

II. EXPERIMENT

Gas-phase fullerene anions were generated according to Hampe *et al.*[13] by electrospray ionization of a 1 mM solution of C_{60} (Sigma-Aldrich) in *o*-dichlorobenzene containing a 100-fold excess of tetrakis-(dimethylamino)ethylene. Ions emanating from the stainless steel desolvation capillary of the home-built electrospray source were guided with a radio-frequency (rf) ion funnel into a cylindrical rf ion trap,[14] which interfaces the cw electrospray ion source to a perpendicularly mounted reflectron time-of-flight (TOF) mass spectrometer operated synchronously with the laser system. In photoelectron spectroscopy mode, reflectron potentials were set to ground and ions passed into the detachment chamber of a TOF photoelectron spectrometer mounted downstream from the reflectron. Using a magnetic bottle[15] to collect and guide the electrons through the photoelectron drift tube allows a collection efficiency of nearly unity. Doppler broadening was reduced by decelerating and electrostatically focusing ion packets before detachment. The typical resolution of our setup was $\Delta E/E \approx 4\%$ for electrons of a kinetic energy of $E_{\mathrm{kin}}=1$ eV. Pump and probe laser pulses were provided by a fully integrated 1 kHz femtosecond system (Clark-MXR, CPA 2001) comprising an Er^{3+} fiber oscillator and a chirped pulse amplification system to yield 775 nm laser pulses of 190 fs (sech^2) pulse length. After second-harmonic generation, the pump (775 nm) and probe (388 nm) laser beams were separated and delayed relative to each other using an optical delay line (Nanomover, Melles Griot). Unfocused pump and probe beams were then collinearly recombined and collimated to a diameter of 3 mm before entering the photodetachment chamber. Here, typical pulse energies were 140 μJ (775 nm) and 20 μJ (388 nm). These intensities were chosen to minimize two-photon processes arising from either only the pump or the probe beams while providing adequate two-color signals. In all measurements, polarization of pump and probe laser beams was perpendicular to each other. Photoelectron spectra were acquired by summing over 2×10^6 single spectra for each pump/probe delay with typical count rates of 100 e/s. The instrumental function, i.e., the temporal cross correlation between the pump and probe pulses, was determined by upconversion in a 50 μm beta-barium borate (BBO) crystal to 280 fs [full width at half maximum (FWHM), see inset of Fig. 4]. Pump/probe scans in this type of experiment are time consuming. Therefore laser drift (pointing stability, intensity) as well as ion beam current fluctuations can present a problem. Such effects were precluded to a large degree by internally referencing the two-color signature to the one-photon detachment signal at 388 nm. From integrated intensities of transient and ground state detachment features, we estimate that at most 4% of all ions in the interaction region were excited by the pump pulse.

III. THEORY

A. Ground state

The ground state geometry of C_{60}^- was optimized within spin-unrestricted density functional theory (DFT) using the B3-LYP functional and a cc-pVTZ basis set, as implemented in the TURBOMOLE program package.[16] As the highest occupied molecular orbital (HOMO) is triply degenerate, the fullerene anion spontaneously undergoes Jahn-Teller distortion.[17–19] Presently, it is not clear whether this Jahn-Teller (JT) effect is of a static or dynamic nature. In the first case, coupling to the A_g and H_g vibrational modes leads to symmetry reduction from I_h to either D_{2h}, D_{3d}, or D_{5d} symmetry.[20] Earlier calculations indicated that the D_{3d} structure is a minimum, whereas D_{5d} and D_{2h} forms were found to be maxima/saddle points.[17,18] Note, however, that the overall JT instabilities were found to be only on the order of a few kJ/mol. Correspondingly, orbital shifts and differences in electronic excitation energies relative to the I_h structure are small. For the purposes of this study, calculations were symmetry restricted to the D_{3d} point group allowing for elongation of the fullerene cage along the C_3 axis.

B. Excited states

Electronic excitations within the range up to 2.6 eV were calculated using the same basis set and functional by means of time-dependent density functional theory (TDDFT). This has proven to be an adequate method for fullerenes in various charge states.[22–24] The B3-LYP functional is a compromise in the sense of minimization of self-interaction effects due to the use of an exact exchange functional on the one hand and treatment of electron correlation with an additional semiempirical functional on the other hand. Additionally, low-lying excited states were calculated using coupled cluster theory within the approximation of the resolution of the identity. Results coincide well with TDDFT energies and support an error assessment of ca. ±100 meV.[22] Excitation energies and term symbols obtained from TDDFT are shown in Fig. 1. The irreducible representations of the single particle states and transitions (shown on the right side) are those of neutral C_{60} in the undisturbed I_h symmetry. The only state accessible via dipole allowed one-photon excitation from the ground state of the negative ion is drawn in black. Dipole-forbidden states are shown in gray.

Upon one-electron occupation and static JT distortion, the t_{1u} lowest unoccupied molecular orbital of neutral C_{60} splits up into the lower a_{2u} and the e_u orbitals. The first excited $\tilde{A}^-$ state of C_{60}^- arises from a transition between the latter orbitals. This is associated with a low excitation energy of 0.15 eV. In the case of dynamic JT effect, the $\tilde{X}^-$ and $\tilde{A}^-$

Downloaded 23 Aug 2008 to 134.147.252.238. Redistribution subject to AIP license or copyright; see http://jcp.aip.org/jcp/copyright.jsp

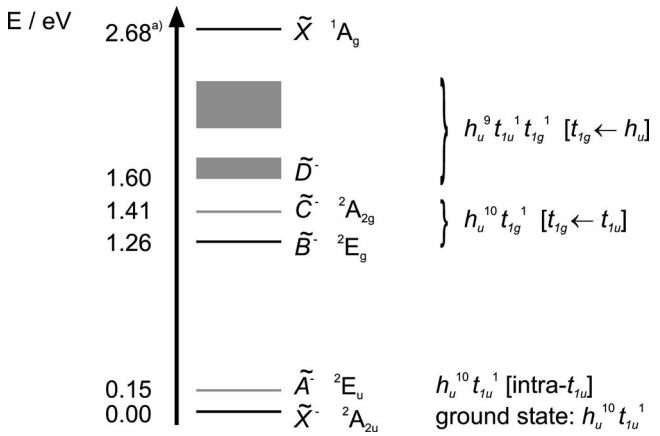


FIG. 1. Doublet electronic states of geometrically relaxed C_{60}^- (D_{3d} symmetry) and the singlet ground state of C_{60} as obtained from TDDFT calculations. The $\tilde{B}^-(^2E_g)$ state of the anion is accessible via a dipole allowed transition from the ground state. Dark states are drawn in gray. The superscript "a)" represents the adiabatic electron affinity taken from Wang *et al.* (Ref. 21).

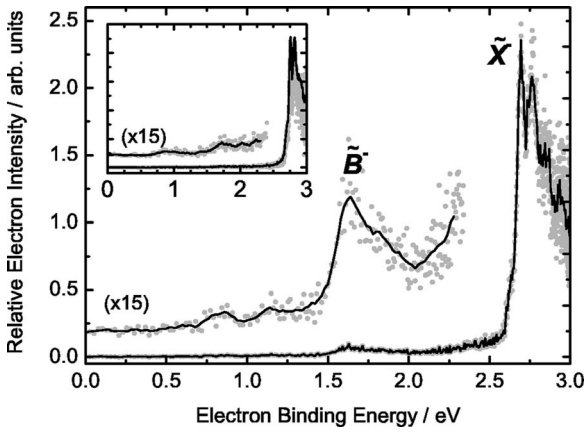


FIG. 2. Pump/probe photoelectron spectrum with 1.6 eV pump and 3.2 eV probe pulses at zero delay. Inset: Photoelectron spectrum of C_{60}^- obtained with the 3.2 eV probe pulse only.

states are vibronic states and will interconvert on the time scale of the JT active vibrations. At higher excitation energies, another two states $\tilde{B}^-$ and $\tilde{C}^-$ appear. These derive from the split $t_{1g} \leftarrow t_{1u}$ excitation. While the $\tilde{B}^-$ state can be reached via dipolar electronic excitation ($e_g \leftarrow a_{2u}$), transitions to the higher $\tilde{C}^-$ state ($a_{2g} \leftarrow a_{2u}$) are dipole forbidden. The calculated $\tilde{B}^-$ state transition energy of 1.26 eV is in good agreement with the experimental value of 1.16 eV obtained by multiphoton absorption/depletion probes of C_{60}^- in a storage ring.[19] Earlier matrix absorption measurement[25] yielded similar results. However, the interpretation of matrix studies was proven later to be complicated by a polarizability dependent stabilization of particular static JT structures.[26]

As is the case for $\tilde{X}^-$ and $\tilde{A}^-$, the energy difference between $\tilde{B}^-$ and $\tilde{C}^-$ is small and dynamic JT effect would lead to rapid interconversion. Note that for all states $\tilde{X}^-$-$\tilde{C}^-$, the electronic configurations allow only doublet states. To even higher energies, promotion of one electron from h_u-derived orbitals to the set of t_{1u}-derived orbitals leads to a band of 15 electronic states, with a minimum calculated energy of 1.60 eV. All of these states calculated up to 2.6 eV above the ground state are dipole forbidden. The $h_u^9 t_{1g}^1 t_{1u}^1$ configuration contains nominally three unpaired spins and thus both doublet and quartet configurations are possible. According to Hund's rule, the latter can be expected to be slightly lower in energy than the corresponding doublet states.

IV. RESULTS

A. Overview and general remarks

Figure 2 shows the photoelectron (PE) spectrum of C_{60}^- upon two-color (388+775 nm) irradiation at a pump/probe delay of $\Delta t=0$ ps. This can be compared with the inset which shows the photoelectron spectrum obtained with only 388 nm (probe) excitation and the same probe pulse intensity. Purely pump irradiation does not lead to measurable photoelectrons. The peak at 2.69±0.05 eV electron binding energy ($\tilde{X}^-$) stems from direct detachment of the negative ion with one probe photon—consistent with the known electron affinity of C_{60}^- (2.683±0.008 eV).[21] Features at higher electron binding energies reflect the generation of vibronically excited ground state neutrals (with one or more quanta of A_g and/or H_g vibrations excited[21,27,28]). The intensity of these transitions and the existence of hot bands on the left side of the vertical detachment feature indicate that the fullerene ions are at about room temperature or slightly above.[21] The feature labeled $\tilde{B}^-$ in Fig. 2 at an electron binding energy of 1.63±0.05 eV is only observed under two-color irradiation and scales linearly with the pump pulse intensity. It is due to absorption of one pump photon followed by detachment of the excited state with a probe photon. We base this assignment on the observed shift of $\tilde{B}^-$ relative to the adiabatic electron affinity (the $\tilde{X}^-$ feature) of $\Delta E=1.1\pm0.1$ eV. This is in good quantitative agreement with the experimentally determined excitation energy of the $\tilde{B}^-(^2E_g)$ state by photodepletion (1.16 eV).[19] The above interpretation implies that the energy mismatch of 0.5 eV between the pump photon energy and the pure electronic excitation energy of the $\tilde{B}^-(^2E_g)$ state is being pumped into kinetic energy of the nuclei in a vibronic transition. As the fullerene cage is rather rigid, vertical photodetachment transitions are preferred which do not lead to significant changes in vibrational excitation. Consequently, at the resolution of our experiment, the kinetic energy distribution of the detached electrons should remain essentially unaffected by the level of $\tilde{B}^-(^2E_g)$ state vibrational excitation.

The weak features in Fig. 2 at electron binding energies higher than the $\tilde{B}^-$ state and the intensity of the $\tilde{B}^-$ state signal in the inset of Fig. 2 scale to the square of the probe pulse energy and are not affected under variation of the pump pulse intensity. Therefore each of them can be attributed to a pump/probe process induced by 388 nm radiation with an internal conversion process in between the photoinduced steps. The observation of all these features indicates an ultrafast internal conversion relaxation of the higher excited doublet (?) states of C_{60}^- on the time scale of the autocorrelation of the probe laser pulse (~280 fs) or faster.

Downloaded 23 Aug 2008 to 134.147.252.238. Redistribution subject to AIP license or copyright; see http://jcp.aip.org/jcp/copyright.jsp

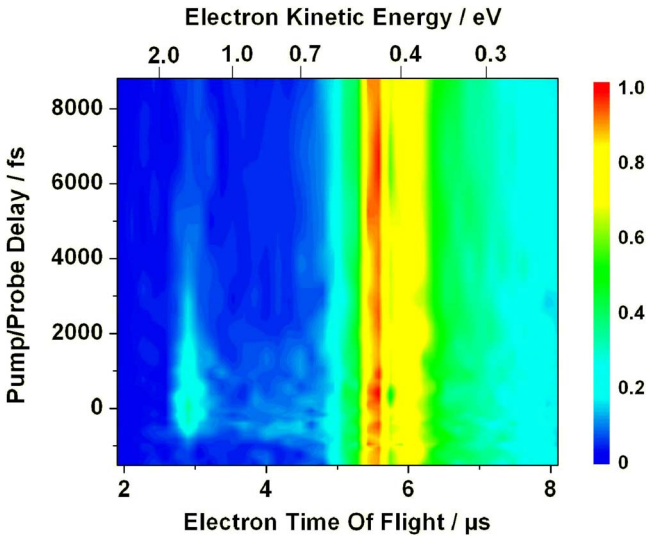


FIG. 3. (Color online) Contour plot of pump/probe photoelectron spectra at various pump/probe delay times. The spectra are drawn vs electron time of flight for better visualization of the transient feature.

Variation of the pump/probe delay yields the spectra shown in the contour plot in Fig. 3. For clarity, all spectra are plotted in the electron TOF domain.[35] Spectra were normalized to the intensity of the ground state detachment feature at about 6 μs eTOF.

While the decay of the transient $\tilde{B}^-$ state can be observed at a time of flight of around 3 μs followed by a weak tail up to eTOF as high as ~4.8 μs, no further time-dependent signal is visible, especially no transients gaining intensity on a similar time scale.

Figure 4 shows the integrated $\tilde{B}^-$ state intensity in the range between 1.5 and 1.9 eV electron binding energies at various pump/probe delays. To obtain this from the data shown in Fig. 3, a constant contribution from time-independent background signal (from very large negative up to very large positive pump/probe delay times) of <5% of the $\tilde{B}^-(^2E_g)$ state peak intensity at zero delay was subtracted. It was assigned to result from two probe-photon induced detachment and electronic noise. The continuous line is a fit of a single exponential decay beginning at zero time as shown in Eq. (1) convoluted with a Gaussian of τ_{instr} =280 fs width (FWHM), to account for the temporal resolution of the experiment.

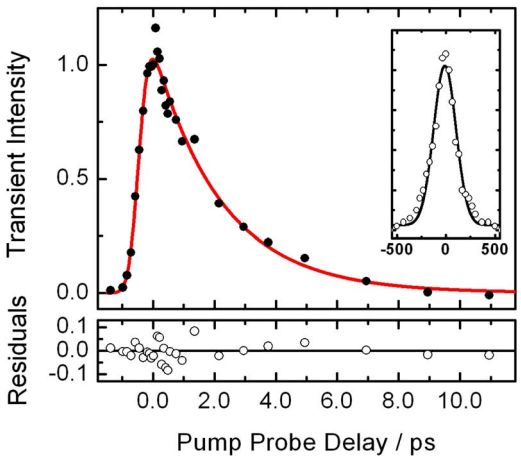


FIG. 4. (Color online) Temporal evolution of the integrated transient detachment feature. Black dots are experimental data; the line is a fit to a single exponential decay, convoluted with the instrumental function. The inset shows the cross correlation of the pump/probe pulses as measured by up-conversion in 50 μm BBO. Units on the abscissa of the inset are femtoseconds.

$$\frac{I(\Delta t)}{I_0} = \int_0^\infty \exp\left\{-\left(2\sqrt{\ln 2}\frac{t-\Delta t}{\tau_{\text{instr}}}\right)^2\right\}\exp\left\{-\frac{t}{\tau_{\text{el}}}\right\}dt. \quad (1)$$

Least square fitting results in a decay time of τ_{el} =2.2±0.2 ps. The residuals as the difference between the integrated intensities and the least square fit in the lower part of Fig. 4 do not show any systematic time dependency, supporting the single exponential dynamics. Their maximum value corresponds to the statistical error. No further transient features were observed in the photoelectron spectra up to pump/probe delays of tens of picoseconds, indicating that longer lived states are not populated to a significant extent. Heating of the ground state after conversion of the electronic excitation energy into cage vibrations was not apparent at the presently achievable signal-to-noise ratio.

B. Relaxation mechanism

Weak fluorescence in the near infrared (NIR) has been observed for electrochemically generated C_{60}^- in solution[29] after excitation at 1064 nm. However, no quantum yield has been reported. Calculating an inverse Einstein coefficient of 300 ns from the electronic transition dipole moment between $\tilde{X}^-$ and $\tilde{B}^-$ states,[30] radiative decay can be excluded as a substantial relaxation pathway. Furthermore, the corresponding *picosecond* lifetime is much too short to be associated with intersystem crossing (moreover, our spectra do not show features arising from long-lived states). Consequently, we infer that the $\tilde{B}^-$ state decays predominantly by fast non radiative relaxation into the electronic ground state. This is in contrast to C_{60} for which excitation at the absorption onset (somewhat higher in energy than for C_{60}^-) leads to the population of singlet states which relax predominantly by way of intersystem crossing to the triplet manifold. We tentatively exclude internal conversion to the first excited $\tilde{A}^-$ state, as no corresponding transient detachment features can be observed in the photoelectron contour plot (Fig. 3). However, we cannot completely rule out a relaxation to this state followed by further ultrafast decay to the electronic ground state, which would also suppress the observation of a transient feature by minimizing the $\tilde{A}^-$ state population at any given time.

According to the standard theory of intramolecular radiationless transitions in isolated large molecules as first proposed by Bixon and Jortner,[31] the excitation process can be described as the generation of a wave packet $|\Psi(t=0)\rangle$ comprising the first-order states generated through the coupling of the initially populated vibronic zero-order state φ_s (with the electronic configuration of the adiabatic $\tilde{B}^-$ state) to the dark quasicontinuum of vibronic states $\{\varphi_i\}$ belonging to another electronic configuration (*here*: the electronic ground state $\tilde{X}^-$). The decay time of the $\tilde{B}^-$ state can then be ex-

Downloaded 23 Aug 2008 to 134.147.252.238. Redistribution subject to AIP license or copyright; see http://jcp.aip.org/jcp/copyright.jsp

tracted from the single exponential decay of the squared projection of the wave packet onto the zero-order state φ_s: $P(t)=|\langle\varphi_s|\hat{S}\Psi(0)\rangle|^2=|\langle\varphi_s|\Psi(t)\rangle|^2$ with the propagator $\hat{S}$. It turns out that the associated internal conversion rate is proportional to the averaged coupling matrix element $\nu=\langle\nu_i\rangle$ (with $\nu_i=\langle\varphi_s|\hat{H}|\varphi_i\rangle$) squared times the vibrational state density ϵ^{-1} of the final state (at the total internal energy after excitation). Both necessary conditions for the validity of the Jortner and Bixon model, a greater bandwidth of the excitation pulse than the linewidth of the transition to the first-order states, and a larger vibronic coupling ν than the reciprocal density of vibrational states ϵ in the accepting quasicontinuum, are fulfilled in our measurements. On the basis of the Haarhoff approximation[32] and DFT-derived vibrational frequencies[33] we calculate the vibrational state density of C_{60}^- at a total internal energy corresponding to the pump photon energy plus a room temperature vibrational energy average minus the zero-point energy to be $4\times10^{27}/\mathrm{cm}^{-1}$. The observed relaxation rate then yields a vibronic coupling matrix element of $\nu=1.0\times10^{-14}$ cm^{-1}. This can be compared to an analogously derived number for the S_0-S_1 (1.94 eV) coupling of room temperature C_{60}. Here, the observed ISC rate[1,2,6] provides an upper limit to the internal conversion rate from which we infer that $\nu'\leqslant1.1\times10^{-17}$ cm^{-1}. Apparently, the lowest singlet excited state of C_{60} is much less strongly coupled to its electronic ground state than is the C_{60}^- state. Highly efficient electronic to vibrational coupling has also been proposed in theoretical treatments of JT distorted fullerene anions contained within superconducting doped fulleride solids.[27,34] Note that the vibronic coupling constant ν contains the averaged squared Franck-Condon overlap of the vibrational wave functions involved. We therefore propose the larger coupling in the case of the negatively charged fullerene (where both $\tilde{B}^-$ and $\tilde{X}^-$ states are subject to Jahn-Teller distortion) is due to the activation of the eight H_g modes. This is in contrast to the neutral molecule with a closed shell electronic ground state, leading to a much smaller subspace of accepting vibrational mode configurations.

In future experimental work on isolated C_{60}^- it will be of interest to study $\tilde{X}^-$-$\tilde{B}^-$ coupling as a function of excess vibrational excitation. In this context an accurate computational determination of the lowest quartet state energy is desirable.

V. CONCLUSIONS

In summary, we have measured pump/probe photoelectron spectra of mass-selected, near room temperature C_{60}^- in the gas phase. The lifetime of the vibrationally excited $\tilde{B}^-(^2E_g)$ state at an energy of 1.26 eV was found to be $\tau=2.2\pm0.2$ ps. The dominant decay process corresponds to intramolecular radiationless transitions into ground state C_{60}^-. The averaged vibronic coupling matrix element to the electronic ground state was calculated to be $\nu=1.0\times10^{-14}$ cm^{-1}, about three orders of magnitude larger than the coupling of the lowest singlet excited state to its ground state in neutral C_{60}.

ACKNOWLEDGMENTS

This research was supported by the Deutsche Forschungsgemeinschaft as administered by the Karlsruhe Center for Functional Nanostructures.

[1] T. W. Ebbesen, K. Tanigaki, and S. Kuroshima, Chem. Phys. Lett. **181**, 501 (1991).
[2] D. K. Palit, A. V. Sapre, J. P. Mittal, and C. N. R. Rao, Chem. Phys. Lett. **195**, 1 (1992).
[3] V. M. Farztdinov, Y. E. Lozovik, Y. A. Matveets, A. G. Stepanov, and V. S. Letokhov, J. Phys. Chem. **98**, 3290 (1994).
[4] D. Dick, X. Wei, S. Jeglinski, R. E. Benner, Z. V. Vardeny, D. Moses, V. I. Srdanov, and F. Wudl, Phys. Rev. Lett. **73**, 2760 (1994).
[5] A. Sassara, G. Zerza, V. Ciulin, M. T. Portella-Oberli, J.-D. Ganière, B. Deveaud, and M. Chergui, J. Lumin. **83–84**, 29 (1999).
[6] A. Sassara, G. Zerza, M. Chergui, V. Ciulin, J.-D. Ganière, and B. Deveaud, J. Chem. Phys. **111**, 689 (1999).
[7] A. G. Stepanov, M. T. Portella-Oberli, A. Sassara, and M. Chergui, Chem. Phys. Lett. **358**, 516 (2002).
[8] S. B. Fleischer, B. Pevzner, D. J. Dougherty, E. P. Ippen, M. S. Dresselhaus, and A. F. Hebard, Appl. Phys. Lett. **69**, 296 (1996).
[9] E. E. B. Campbell and R. D. Levine, Annu. Rev. Phys. Chem. **51**, 65 (2000).
[10] E. E. B. Campbell, K. Hansen, K. Hoffmann, G. Korn, M. Tchaplyguine, M. Wittmann, and I. V. Hertel, Phys. Rev. Lett. **84**, 2128 (2000).
[11] E. E. B. Campbell, K. Hoffmann, and I. V. Hertel, Eur. Phys. J. D **16**, 345 (2001).
[12] K. Hansen, K. Hoffmann, and E. E. B. Campbell, J. Chem. Phys. **119**, 2513 (2003).
[13] O. Hampe, M. Neumaier, M. N. Blom, and M. M. Kappes, Chem. Phys. Lett. **354**, 303 (2002).
[14] D. Gerlich, Hyperfine Interact. **146**, 293 (2003).
[15] P. Kruit and F. H. Read, J. Phys. E **16**, 313 (1983).
[16] R. Ahlrichs, M. Bär, M. Häser, H. Horn, and C. Kölmel, Chem. Phys. Lett. **162**, 165 (1989).
[17] N. Koga and K. Morokuma, Chem. Phys. Lett. **196**, 191 (1992).
[18] W. H. Green, S. M. Gorun, G. Fitzgerald, P. W. Fowler, A. Ceulemans, and B. C. Titeca, J. Phys. Chem. **100**, 14892 (1996).
[19] S. Tomita, J. U. Andersen, E. Bonderup, P. Hvelplund, B. Liu, S. B. Nielsen, U. V. Pedersen, J. Rangama, K. Hansen, and O. Echt, Phys. Rev. Lett. **94**, 053002 (2005).
[20] A. Ceulemans, J. Chem. Phys. **87**, 5374 (1987).
[21] X. B. Wang, H. K. Woo, and L. S. Wang, J. Chem. Phys. **123**, 051106 (2005).
[22] R. Bauernschmitt, R. Ahlrichs, F. H. Hennrich, and M. M. Kappes, J. Am. Chem. Soc. **120**, 5052 (1998).
[23] O. T. Ehrler, J. M. Weber, F. Furche, and M. M. Kappes, Phys. Rev. Lett. **91**, 113006 (2003).
[24] O. T. Ehrler, F. Furche, J. M. Weber, and M. M. Kappes, J. Chem. Phys. **122**, 094321 (2005).
[25] J. Fulara, M. Jakobi, and J. P. Maier, Chem. Phys. Lett. **211**, 227 (1993).
[26] H. Kondo, T. Momose, and T. Shida, Chem. Phys. Lett. **237**, 111 (1995).
[27] O. Gunnarsson, H. Handschuh, P. S. Bechthold, G. Kessler, B. Ganteför, and W. Eberhardt, Phys. Rev. Lett. **74**, 1875 (1995).
[28] X. B. Wang, C. F. Ding, and L. S. Wang, J. Chem. Phys. **110**, 8217 (1999).
[29] T. Kato, T. Kodama, and T. Shida, Chem. Phys. Lett. **205**, 405 (1993).
[30] R. C. Hilborn, Am. J. Phys. **50**, 982 (1982).
[31] M. Bixon and J. Jortner, J. Chem. Phys. **48**, 715 (1968).
[32] P. C. Haarhoff, Mol. Phys. **7**, 101 (1963).
[33] J. Menéndez and J. B. Page, in *Light Scattering in Solids VIII*, edited by M. Cardona and G. Güntherodt (Springer, Berlin, 2000).
[34] Y. Asai and Y. Kawaguchi, Phys. Rev. B **46**, 1265 (1989).
[35] As the relation between electron TOF and kinetic energy is nonlinear, conversion to the energy domain is accompanied with a Jacobi transformation, relatively emphasizing the high TOF or low kinetic energy part of the spectrum.

Downloaded 23 Aug 2008 to 134.147.252.238. Redistribution subject to AIP license or copyright; see http://jcp.aip.org/jcp/copyright.jsp